Hybrid Formation of Carboxypeptidase A and Fraction II of Procarboxypeptidase A*

William D. Behnke,† David C. Teller, Roger D. Wade, and Hans Neurath‡

ABSTRACT: Fraction II, the endopeptidase subunit of bovine procarboxypeptidase A, combines spontaneously with carboxypeptidase A (Cox) to yield a 1:1 hybrid displaying carboxypeptidase activity. Verification of the stoichiometry of this association has been obtained by Job's method of continuous variations and high-speed sedimentation equilibrium experiments submitted to computer analysis. These data have yielded a K_{assoc} of 2.9×10^4 l./mole. The effects of protein concentration, temperature, ionic strength, and pH have been ascertained by sedimentation velocity experiments. In addition, since both fraction II and carboxypeptidase A are stable in solution, they have been chemically modified separately and tested for their ability to form a hybrid. In this respect, metal ion substitution, incubation with inhibitors such as β-phenylpropionate, and acetylation with *N*-acetylimidazole have not prevented carboxypeptidase A from forming a hybrid, nor has incubation with substrates or inhibitors of fraction II prevented its ability to react. Of the modifications performed, only succinylation of fraction II and cyanoethylation of carboxypeptidase A have abolished hybridization. In general, the data favor the participation of ionic forces in forming the hybrid and thus suggest their involvement in the subunit interactions of procarboxypeptidase A.

Recent studies on the isolation and physical properties of bovine procarboxypeptidase A have shown that this zymogen exists in at least two major forms: PCP A-S6[1] which is an aggregate of three subunits, and PCP A-S5, an aggregate of subunits I and II comprising approximately 20–25% of the total zymogen present in extracts of pancreatic glands. Disaggregation of PCP A-S5 by alkaline solutions (pH 10.5) have yielded fractions I and II which have been separated chromatographically and shown to be comparable to fractions I and II isolated from PCP A-S6. Some of the chemical and enzymatic properties have been described by Brown *et al.* (1963).

It was observed that under certain conditions, activation of PCP A-S5 did not lead to disaggregation, suggesting that the structural features of subunit I responsible for binding to subunit II are still present in the activated product. It thus seemed possible that a mixture of CPA and fraction II should combine to form a complex resembling partially activated PCP A-S5. Preliminary data by Brown *et al.* (1963) suggested that this was the case. The purpose of the study presented here was to investigate this association in detail in order to define the stoichiometry precisely and to provide evidence for the specific groups involved in the reaction.

Materials and Methods

PCP A-S6 was isolated from aqueous extracts of acetone powders of bovine pancreas glands and purified by chromatography on DEAE-cellulose, as described by Yamasaki *et al.* (1963). An additional step involving gel filtration on Sephadex G-150 (eluting buffer 0.05 M KH_2PO_4, pH 8.0) was found to yield a more homogeneous preparation. Little change in the specific activity of PCP A-S6 was observed in the material isolated by including this additional purification step, since the contaminating material was largely another form of procarboxypeptidase, PCP A-S5 (R. W. Tye, unpublished experiments). *Fraction II* was prepared according to the method of Brown *et al.* (1963). *Succinyl fraction II* was prepared as described in the preceding paper of this series (Behnke *et al.*, 1970). CPA (Cox) was prepared from procarboxypeptidase according to the procedure of Cox *et al.* (1964). This preparation contains predominantly the α form (Pétra and Neurath, 1970).

Proflavin dihydrochloride dihydrate was purchased from Nutritional Biochemical Corp. It was found to be pure by paper electrophoresis (pyridine–acetate, pH 6.5) and ascending chromatography in 1-butanol–acetic acid–water (4:1:5, v/v) except for a trace of insoluble material remaining at the origin.

Acrylonitrile was purchased from Matheson, Coleman and Bell and redistilled before use. *N-Acetylimidazole* was purchased from the Cyclo Chemical Corp. and recrystallized from isopropenyl acetate. DFP was obtained from the Aldrich

* From the Department of Biochemistry, University of Washington, Seattle, Washington 98105. *Received July 28, 1969.* This work has been supported in part by the Public Health Service, National Institutes of Health (GM 13401 and GM 04617), by the American Cancer Society P-79), the National Science Foundation (GB 4990X), and the Office of Naval Research, Department of the Navy (NONR 477-35).

† Taken in part from a dissertation submitted by W. D. B. to the Graduate School of the University of Washington in partial fulfillment of the requirements for the degree of Doctor of Philosophy. Recipient of a predoctoral training stipend from a training grant by the National Institutes of Health to the Department of Biochemistry (GM 5212). Present address: Biophysics Research Laboratory of the Department of Biological Chemistry, Peter Bent Brigham Hospital, Harvard Medical School, Boston, Mass. 02115.

‡ To whom to address correspondence.

[1] Abbreviations used in this paper are: PCP A-S6, procarboxypeptidase A, 6 S; PCP A-S5, procarboxypeptidase A, 5 S; CPA, carboxypeptidase A; CbzGly-L-Phe, carbobenzoxyglycyl-L-phenylalanine; HPLA, hippuryl-DL-β-phenyllactic acid; TNM, tetranitromethane; DIP, diisopropylphosphoryl.

Chemical Co. HPLA was obtained from Cyclo Chemical Corp. All other materials were standard reagent grades.

Peptidase activity was measured spectrophotometrically according to the procedure of McClure (1964); CbzGly-L-Phe, 3.2×10^{-4} M in 0.05 M Tris–1 M NaCl (pH 7.5), was used as the peptide substrate for carboxypeptidase A. The decrease in absorbance (linear portion) at 223 nm (25°) was followed and the specific activity was expressed as ΔA_{223} $\text{min}^{-1}/\mu\text{g}$ of protein.

Various metal derivatives of carboxypeptidase A were prepared using the methods of Coleman and Vallee (1960). For the preparation of the apoenzyme, CPA was dissolved in 0.1 M Tris-HCl–1 M NaCl (pH 7.0), at 25°, and was dialyzed at 4° for 2 days with several buffer changes against the same buffer containing 2×10^{-3} M *o*-phenanthroline. One aliquot of apoCPA was dialyzed against dithizone-extracted buffer (0.1 M Tris-HCl, pH 7.0) and another against 0.1 M Tris-HCl–2×10^{-3} M *o*-phenanthroline at pH 7.0. Metalloenzymes were made from the apoenzyme by dialysis for 24 hr against 10^{-4} M Hg^{2+} and 10^{-4} M Cd^{2+}–0.1 M Tris-HCl–1 M NaCl (pH 7.0). Excess metal ion was removed by a final dialysis against metal-free 0.1 M Tris-HCl (pH 7.0). In all cases this latter procedure resulted in crystallization of various metallo derivatives. Fraction II was similarly dialyzed first against 0.1 M Tris-HCl–1 M NaCl–2×10^{-3} M *o*-phenanthroline (pH 7.0), and finally against dithizone-extracted 0.1 M Tris-HCl (pH 7.0).

All transfers, measurements, and manipulations were made with materials (including pH-Stat vessels, ultracentrifuge cells, etc.) that were treated with metal-free buffers or doubly glass-distilled water. All assays were carried out with metal-free substrate solutions. Esterase activities for apo-, Hg^{2+}-, and Cd^{2+}-carboxypeptidase were found to be 1.1, 49, and 179%, respectively, of the native Zn^{2+} enzyme, using a rate constant of 0.208 mequiv of OH^-/min per mg (Cox *et al.*, 1964). Measurements of peptidase activity for Hg^{2+}- and Cd^{2+}-carboxypeptidase yielded values of 0.76 and 2.48%, respectively.

Sedimentation velocity analyses were carried out in a Beckman Model E analytical ultracentrifuge equipped with phase-plate schlieren, Rayleigh, and absorption optical systems. The analyses were performed in either a single- or double-sector cell at 60,000 rpm. Plate negatives of the observed schlieren patterns were taken at regular time intervals during the run and the radial boundary position of the maximum ordinate was measured on a microcomparator at each time interval. The sedimentation rate was calculated from a least-squares plot of the log of the radial boundary position *vs.* time (Schachman, 1957).

To facilitate mass transport and maximum ordinate measurements of sedimentation velocity experiments, a T-shaped light source slit was used to record both interference and schlieren patterns simultaneously. This slit is mounted on a brass block which replaces the regular slit jaw blocks. The Rayleigh slit is 6 mm long and 0.15 mm wide and is centered on the optical axis. The schlieren slit extends along the light source axis giving the lower portion of the pattern. The width of this slit is 0.2 mm which permits a good photograph on Kodak II-G plates with a 60–90-sec exposure time for green light (Kodak Wratten 77A filter) and symmetrical upper aperture with a 36-μ slit width. One jaw of each light source slit is adjustable and the edge of the slit has the same height as the standard slits. A somewhat similar slit has recently been described by Massie *et al.* (1968).

For calculations of mass transport, the fringe position in the cell was recorded as a function of the fringe number. These data were processed on a digital computer using a program from Rubin (1966).

Viscosities were measured at 20.00 ± 0.01° and corrections for buffer densities were obtained by pycnometry at 20.0°. Protein concentration, C_0, was calculated by use of a synthetic boundary cell in conjunction with Rayleigh interference optics in the ultracentrifuge. The concentration was calculated from $C = J\lambda/a(dn/dC)$, where J is the number of fringes across the boundary, λ is the wavelength of the Hg line, 5464 Å, a is the length of the light path through the cell (1.2 cm), and dn/dC is the refractive index increment assumed to be 0.00185 dl/g (Doty and Edsall, 1951).

Low-Speed Sedimentation Analysis. Sedimentation equilibrium measurements at 1.8–7.0° were performed in the analytical ultracentrifuge employing Rayleigh interference optics as described by Richards and Schachman (1959) at speeds ranging from 6014 to 10,222 rpm. A double-sector synthetic boundary cell was used to obtain a value of the initial concentration, C_0, and the dialyzed protein sample to be analyzed was layered over FC-43 (3M Chemicals) at column heights of 2.0–2.5 mm. Hingepoint shift was followed in serial patterns. Equilibrium was assumed to be attained when no further shift of the fringes could be detected. The data were plotted as the ln C *vs.* r^2 (where C is the fringe number and r is the distance from the axis of rotation). The apparent weight-average molecular weight, M_w, over the mass of the cell was determined from the total change in the concentration across the cell relative to the initial concentration according to the equation of Lansing and Kraemer (1935). The weight-average molecular weight over the volume of the cell was evaluated by the equation of Adams (1964).

High-Speed Sedimentation Equilibrium Analysis. The experimental method of high-speed sedimentation equilibrium analysis was that described by Yphantis (1964), except that lower speeds and higher initial concentrations were employed (Teller *et al.*, 1969). For all ultracentrifugation experiments the camera lens was focused at the two-thirds plane of the cell (Svennson, 1954, 1956).

Results

Sedimentation Equilibrium of the CPA–Fraction II Complex. Initial low-speed sedimentation equilibrium data at pH 7.5 in 0.038 M KH_2PO_4 and 0.1 M KCl yielded M_w values in the range of 36×10^3 to 41×10^3 g per mole, while the Z-average molecular weights ranged from 59×10^3 to 98×10^3 g per mole. The initial concentrations were varied from 0.8 to 7.5 mg per ml. These experiments indicated complex formation but were not sufficiently accurate for detailed analysis.

In order to obtain a more critical examination of the process, high-speed sedimentation equilibrium experiments were performed. Figure 1 presents the weight- and number-average molecular weight distributions. In Figure 1 the distribution on the left in each case is the fit for a 1:1 complex between fraction II and CPA. The curve fitting analysis

TABLE I: Analysis of High-Speed Sedimentation Equilibrium Data.[a]

Channel	$k_{F_1P_1}$ ($\times 10^{-3}$), M^{-1}	Components	RMS Deviations C	RMS Deviations M_n	RMS Deviations M_w	F_2P_1 RMS Deviations C	F_2P_1 RMS Deviations M_n	F_2P_1 RMS Deviations M_w	F_1P_2 RMS Deviations C	F_1P_2 RMS Deviations M_n	F_1P_2 RMS Deviations M_w
1	14.6	F_1P_1 and F_3	0.013	380	1016	0.021	1743	1933	0.032	2623	2594
2	51.6	F_1P_1	0.015	312	429	0.014	2029	1294	0.024	2897	1901
	0.4	F_1P_1 and F_3	0.009	962	598						
3	30.3	F_1P_1	0.022	2528	2304	0.042	4753	3756	0.051	5594	4314

[a] All other combinations of components gave negative concentrations of some species. F denotes fraction II and P denotes CPA in this table. The weighted-average $k_{F_1P_1}$ of all 1:1 complex formation values is 28.7×10^3 M^{-1}. RMS = root-mean square.

is summarized in Table I. As may be seen from Table I and Figure 1 the best fit of the experimental data was obtained for a single 1:1 complex. If the models are ranked according to the root-mean-square deviations from the observed molecular weight distributions and F denotes fraction II and P denotes CPA, the F_1P_1 or F_1P_1 plus F_3 ranked first. In contrast, however, the model occupying the second rank is not always the same. In Table I, F_1P_1 or F_1P_1 plus F_3 shows the minimum molecular weight deviation for all three cells. However, F_2P_1 has the second best fit for two cells while F_1P_1 plus F_3 occupies this rank for the remaining cell. We conclude that the mechanism of reaction is most consistent with the formation of a 1:1 complex with an equilibrium constant of about 2.9×10^4 l./mole.

The next question which arises is whether the observed molecular weight distributions could be due to a nonhybridizing mixture of self-associating fraction II and CPA monomer. The observed space of molecular weight averages is shown in Figure 2. The straight lines of this graph enclose the "allowed space" for molecular weight moments of a mixture of fraction II, CPA, and a 1:1 hybrid. The salient features of this graph are that the majority of points lie within the three component lines and appear to follow the line joining fraction II and complex. The curved lines in this figure result from a simulation calculation in which complex formation was assumed to be absent (Appendix). It was considered that fraction II self-associates indefinitely with $K = 8.6 \times 10^3$ l./mole. An equimolar mixture of fraction II and CPA was employed and the experimental parameters (temperature, rotor speed, column height, etc.) were set the same as actually used in the centrifuge. The solid line shows the calculated values of M_z *vs.* $1/M_w$, the dashed line represents M_w *vs.* $1/M_n$, and the dotted line gives $2M_w - M_z$ *vs.* $2/M_n - 1/M_w$ (Yphantis and Roark, 1969; Teller *et al.*, 1969). These predicted curves follow the CPA-fraction II line over a large part of their length, a result demonstrating that additional molecular species are present in these solutions.

From the data presented in Figures 1 and 2 and Table I, the best model of the system is that of 1:1 complex formation together with self-association of fraction II. However, the second best model is the formation of an F_2P_1 complex. This stoichiometry also seems plausible because it approximates the structure of PCP A-S6 (Behnke *et al.*, 1970). In order to definitely prove that a 1:1 complex was being formed, an experiment was performed employing Job's method of continuous variations.

Stoichiometry of the Formation of Complex by Sedimentation Velocity Analysis. As presented in the theoretical section (Appendix) it is possible to apply Job's method of continuous variations in spite of the self-association of fraction II (Teller, 1970). Equimolar concentrations of fraction II and CPA

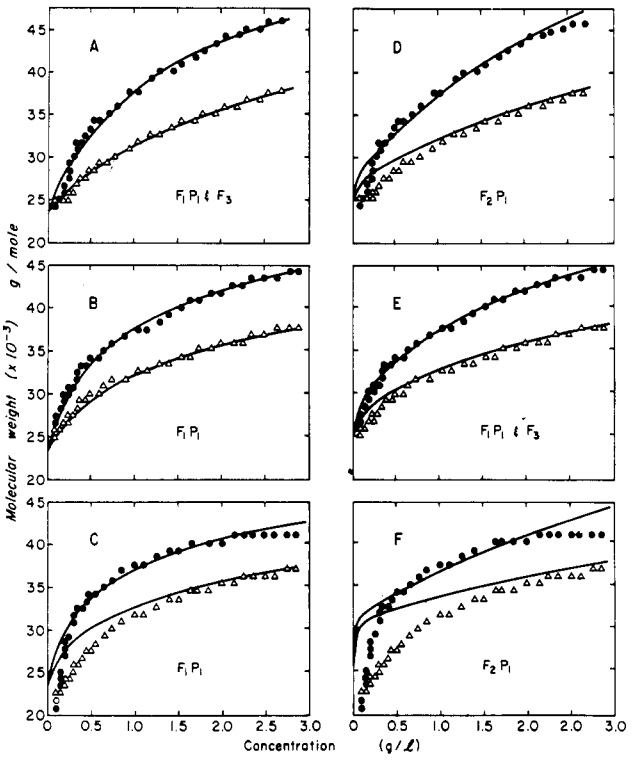

FIGURE 1: Observed and predicted number- and weight-average molecular weights from a high-speed sedimentation equilibrium experiment. The deviations of the points from the theoretical lines are given in Table III. The left side of this figure shows the results for the best fitting model (F_1P_1 and F_3 or F_1P_1). The right panel shows the shape of the distributions for the second best fit to the data. The second best models are F_2P_1 (top), F_1P_1 plus F_3 (middle), and F_2P_1 (bottom); (○) M_w data, (△) M_n data.

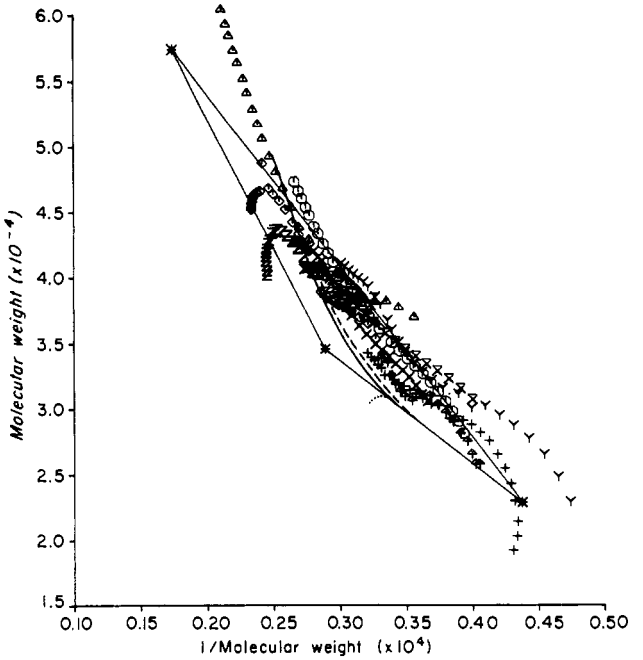

FIGURE 2: "Allowed space" of molecular weights for F_1 = 22.9 × 10^3 g/mole, P_1 = 34.6 × 10^3 g/mole, and F_1P_1 = 57.5 × 10^3 g/mole. The mixture of CPA and fraction II which self-associates are represented by the curved lines. (——) M_w *vs.* $1/M_n$, (- - -) M_Z *vs.* $1/M_w$, (· · ·) $2M_w - M_Z$ *vs.* $2/M_n - 1/M_w$. Hybrid formation is demonstrated by the fact that the points do not follow these curves. Only data from a *y* displacement above one fringe are plotted on the graph. Points outside the triangle of solid lines indicate a departure from the F_1, P_1, and F_1P_1 model.

Table of Symbols

Channel No.	M_Z *vs.* $1/M_w$	M_w *vs.* $1/M_n$	$2M_w - M_Z$ *vs.* $2/M_n - 1/M_w$
1	△	○	+
2	◇	×	⏄
3	Z	⧖	Y

were mixed in the ratio of (*x*) and (1 − *x*) ml of each and sedimented in the ultracentrifuge at 60,000 rpm.

The sedimentation was monitored using both schlieren and Rayleigh systems, and the *s* rate for the system determined using mass transport and equivalent boundary calculations. The data are presented in Figure 3. All experimental points represent average values. Both experimental data and a theoretical curve are represented. The theoretical curve was calculated using an equilibrium constant (2.9 × 10^4 l./mole) determined from high-speed sedimentation equilibrium data and the computed value for the sedimentation coefficient of the complex (s_c) of 4.3 ± 0.2 S. The curve passes through a maximum at mole fraction approximately 0.5, and therefore indicates a 1:1 stoichiometry for complex formation. Calculation of the theoretical mole fraction at the maximum ordinate from eq 8 (Appendix) using these parameters and the constant for indefinite self-association of fraction II of 8.6 × 10^3 M^{-1} predicts the point of maximum ordinate should be x = 0.57 rather than exactly 0.50.

Investigation of System Variables Using Sedimentation Velocity. A sedimentation velocity pattern of a mixture

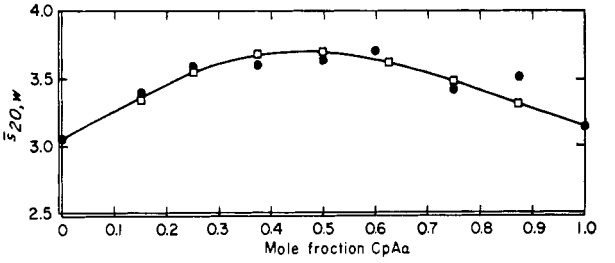

FIGURE 3: Job plot of weight average sedimentation coefficients. C_0 was 1.3 × 10^{-4} M. The points (○) are averages of mass transport and equivalent boundary calculations. The predicted curve (□) is for a 1:1 complex with k_a = 2.9 × 10^4 M^{-1}, s_{FII} = 3.06 S, s_{CPA} = 3.15 S, and $s_{complex}$ = 4.3 S.

containing CPA (in excess) and fraction II is shown in Figure 4. Two major components are present, the faster of which is moving with an *s* rate of 4.22 S and represents the peak containing complex; the slower component apparently consists of excess CPA ($s_{20,w}$ = 3.2 S).

Since crystals were added, in excess of solubility, CPA would dissolve in buffer alone according to its solubility product. This phase equilibrium would be independent of the formation of complex as long as not all the crystals had dissolved. Thus, excess CPA probably accounts for most of the slow-moving boundary in Figure 4 while the products of any dissociated complex account for the remainder.

Figure 5 illustrates the concentration dependence of complex formation. In this case, fraction II and CPA were mixed in equimolar concentrations and portions of this stock solution were diluted prior to ultracentrifugation (C_0 varying from 28.96 to 5.23 fringes). The runs were followed in the optical system which simultaneously records schlieren and Rayleigh patterns. The interference patterns were used to calculate *s* values in which equivalent boundary and mass transport equations are applied rather than the movement of the maximum ordinate. The values of $s_{20,w}$ are 3.94, 3.30, and 3.03 S for maximum ordinate, equivalent boundary, and mass transport calculations, respectively. The maximum ordinate values were consistently higher than those determined by the mass transport and equivalent boundary methods since the latter take into account any slower material present. The fact that the slope of the plot is flat does not mean that there is no concentration dependence. In this case it is likely that the plot is a summation of nonideality (backward flow and viscosity) and inhomogeneity (slow and fast components) which operate in opposite directions such that the net effect is a linear relationship of *s* and *C* with zero slope.

A plot of the sedimentation coefficient, $s_{20,w}$, of the heavy component as a function of temperature is also invariant within the experimental error of measurement, and from this it can be concluded that there is no observable shape change of the complex with temperature. In addition, the distribution of material between slow- and fast-moving components was also independent of temperature.

There is little effect of pH within the range of enzyme stability, *i.e.*, between pH 6.5 and 8.5 as indicated by the *s* rate of the fast component (s_{20} = 3.8–4.0 S and the per cent distribution of material in the slow- and fast-moving boundaries). Higher or lower pH values could not be investigated

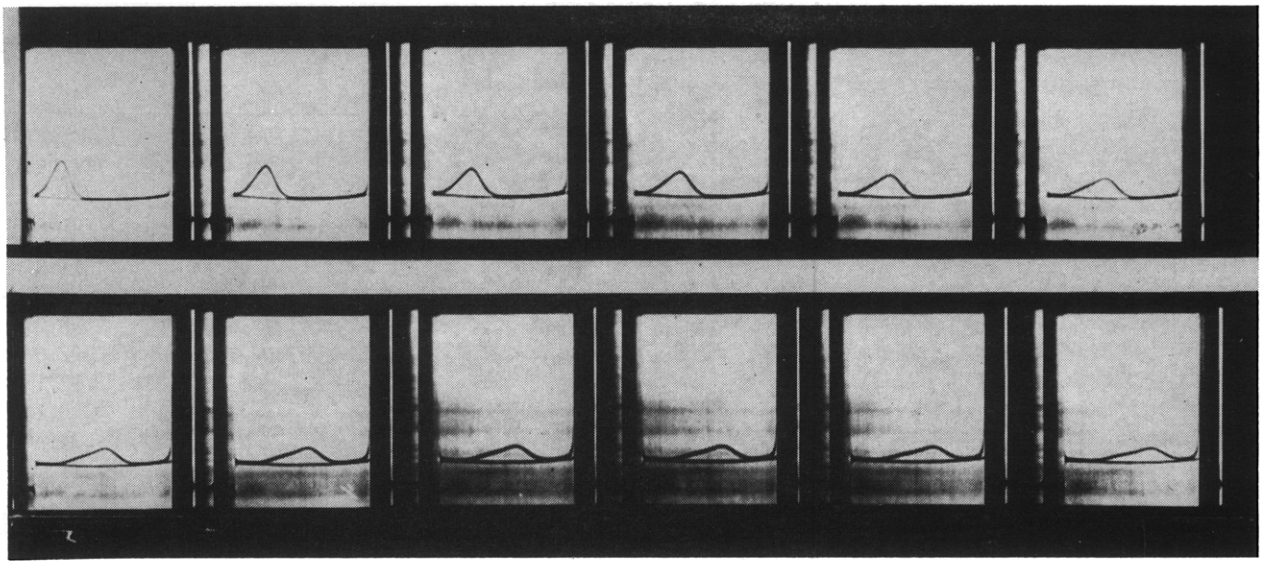

FIGURE 4: Sedimentation velocity of a mixture of CPA (in excess) and fraction II. Exposures of plate A were taken at 16-min intervals. Exposure 1 of plate B was taken at 104 min and the remaining pictures at 8-min intervals. $s_{20,w}$ of the major peak is 4.22 S, 59,987 rpm at 3.1° in 0.038 M KH_2PO_4–0.1 M KCl (pH 7.5), bar angle 70°.

due to denaturation. High ionic strength ($\Gamma/2$ = 1.0 M) causes some broadening of the velocity pattern and decreases the per cent of fast component. Low ionic strengths ($\Gamma/2$ = 0.05 M being the lowest ionic strength tested) were not investigated since primary charge effects might predominate. In general, buffer conditions leading to maximum complex formation were found to be 0.03 M KH_2PO_4 and 0.1–0.2 M KCl (pH 7.5; $\Gamma/2$ = 0.2–0.3 M).

Effects of Substrates and Reversible Inhibitors of Both CPA and Fraction II. Preliminary sedimentation experiments indicated that proflavin, a competitive inhibitor of trypsin and chymotrypsin, interacts with either the activated (endopeptidase) or zymogen forms of PCP A-S6 and fraction II. Additional evidence for this interaction was obtained from kinetic data.

Proflavin inhibits the hydrolysis of Ac-L-TyrOEt by both activated PCP A-S6 and activated fraction II. The relevant data for activated fraction II plotted according to Dixon and Webb (1964) are shown in Figure 6. Inhibition appears to be noncompetitive below 0.01 mM proflavin, the calculated values of K_i being 0.88 for activated PCP A-S6 and 1.0 mM for activated fraction II. At higher proflavin concentrations (0.166 mM), however, the inhibition appears to be mixed (*i.e.*, changes in both V_{max} and K_m). This mixed inhibition becomes quite marked at dye concentrations higher than 0.2 mM (W. D. Behnke, unpublished data).

In preparation for additional ultracentrifuge experiments employing the Model E scanning system, a spectrophotometric investigation was initiated to determine the spectral effects of dye binding to PCP A-S6. This was done by maintaining a constant proflavin concentration (1.85 mM in 0.2 M KH_2PO_4, pH 7.6) and varying the concentration of PCP A-S6 (2.58, 5.16, 10.32, and 15.48 g per l.). The mixtures

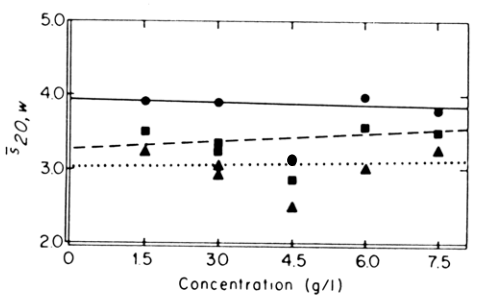

FIGURE 5: Concentration dependence of complex formation determined by sedimentation velocity. An equimolar mixture of fraction II and CPA of 7.5 g/l. was diluted with buffer (0.038 M KH_2PO_4–0.2 M KCl, pH 7.5) prior to ultracentrifugation. (○) Maximum ordinate calculations, $s_{20,w}$ = 3.94 ± 0.09 S (1 − (0.002 ± 0.005)*C*). (□) Equivalent boundary calculations $s_{20,w}$ = 3.30 ± 0.13 S (1 + (0.010 ± 0.008)*C*); (△) mass-transport calculations, $s_{20,w}$ = 3.03 ± 0.17 S (1 + (0.004 + 0.012)*C*). The low points at 4.5 g/l. were not included in the *s vs. C* calculations.

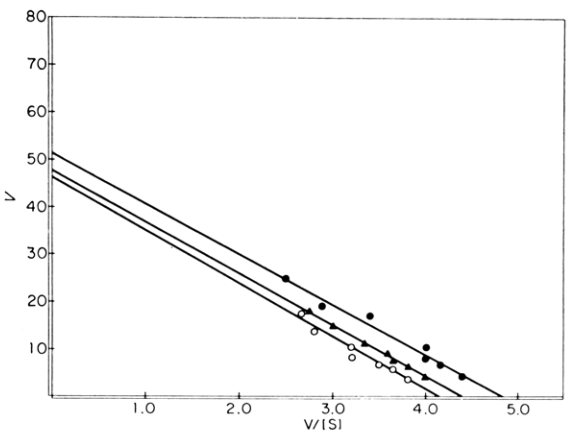

FIGURE 6: Proflavin inhibition by activated fraction II. *V* is given in μl of OH^- (0.1 M base)/min per 20 μl of enzyme solution. The enzyme concentration was 3.30 mg/ml. The substrate concentration varied from 0.005 to 0.1 M; (●) absence of proflavin; (△) 0.085 mM proflavin; (○) 0.166 mM proflavin.

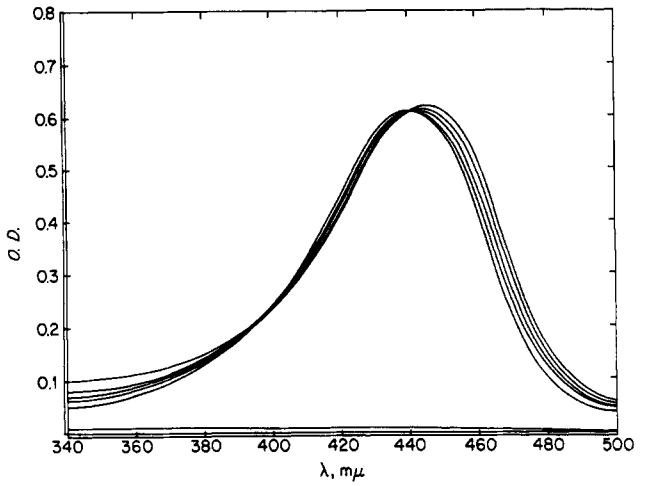

FIGURE 7: Determination of the isosbestic points for proflavin binding to PCP A-S6. Proflavin was maintained constant at 1.85 × 10^{-3} M in 0.2 M KH_2PO_4 (pH 7.6). Protein concentrations varied from 2.58 to 15.48 mg per ml.

of the zymogen and proflavin were scanned in the Cary Model 15 spectrophotometer in the visible region of the spectrum (25°, 0.1-cm cell). The resulting family of curves is shown in Figure 7. Binding of proflavin to PCP A-S6 results in an increasing red shift with increasing protein concentration. Two isosbestic points were observed, one at 440 nm, the maximum absorption of the free dye under these conditions, and another at 395 nm. The former wavelength was chosen in the ultracentrifuge scanning system to follow the movement of proflavin in the centrifuge cell. The binding of proflavin to the protein establishes a concentration gradient of the dye during sedimentation, and the resulting complex migrates with a sedimentation rate approximating that of the protein (Steinberg and Schachman, 1966). From the scanner tracings a sedimentation rate of the migrating boundary was determined. The s value for a mixture of fraction II and CPA (excess CPA crystals) calculated from absorption runs is $s_{20,w}$ = 3.94 ± 0.09 S. This value is higher than the mass transport (3.03 S) and equivalent boundary data (3.30 S) due to the fact that in the absorption system one is following the movement of proflavin, and hence, the movement of fraction II. Due to the presence of excess CPA, fraction II is driven predominantly to complex by mass action, so that the s rate would be expected to correspond more closely to the sedimentation coefficient of the heavy component (s_0 = 4.3 ± 0.2 S calculated from the Job plot). Thus, the experiment indicates that proflavin, and therefore, fraction II, migrates with an s rate more nearly characteristic of PCP A-S5 ($s_{20,w}$ = 5.0 S). The lack of a double proflavin boundary (slow and fast moving) further suggests that the slow boundary can be attributed largely to excess CPA which does not bind proflavin significantly.

β-Phenylpropionate, a competitive inhibitor of CPA at a concentration of 0.05 M, has no effect on complex formation as judged by both the s rate of the heavy component in sedimentation velocity measurements ($s_{20,w}$ = 3.64 S) and the equilibrium constant determined from high-speed sedimentation equilibrium experiments.

As judged by sedimentation velocity experiments, the synthetic substrate for fraction II, Ac-L-TyrOEt, fails to disrupt the association of fraction II and CPA to form a complex as do a number of buffer ions including succinate, Tris-HCl, and bicarbonate. Furthermore, Ac-L-TyrOEt does not displace proflavin from fraction II. However, it is not known whether Ac-L-TyrOEt binds to fraction II (zymogen), and, furthermore, the K_m for Ac-L-TyrOEt is one order of magnitude higher than the K_i for proflavin (Behnke *et al.*, 1970). Lastly, though fraction II can only be partially activated, most of the molecules appear competent with respect to complex formation; therefore, the fractional enzymatic activity does not appear to bear any direct relationship to subunit interactions.

Effects of Modification of Fraction II on Complex Formation. Activation of fraction II under standard conditions (*i.e.*, 0°, 1:100 w/w, trypsin–fraction II, 1 hr) before or after mixing with CPA had no effect upon the complex system. The $s_{20,w}$ of the fast component before activation was 3.74 S and for the activated species 3.73 S. The per cent distribution of material in slow- and fast-moving boundaries was identical in each case. Preparation of the DIP derivative of fraction II, likewise, had no effect upon its ability to form a complex with CPA. In view, however, of the limited extent of activation that can be achieved with fraction II (Behnke *et al.*, 1970), any effect of activation on complex formation would be expected to be relatively small.

Cyanoethylation of fraction II was carried out under conditions similar to those published by Riehm and Scheraga (1966). Fraction II (C = 4.24 g/l.) was dissolved in 0.019

TABLE II: Amino Acid Composition of Cyanoethylated Fraction II.[a]

Amino Acids	Fraction II (Cyanoethyl) 24-hr Hydrolysis	Fraction II (Native) 120-hr Hydrolysis
Lys	3.8	11.3
His	3.5	5.0
Arg	8.0	8.2
Asp	*22.0*	*22.0*
Thr	13.0	12.1
Ser	11.4	9.1
Glu	25.6	24.3
Pro	10.9	11.1
Gly	14.3	15.9
Ala	16.2	15.7
½-Cys	7.2	7.4
Val	15.0	17.0
Met	1.6	1.4
Dicarboxyethyl-Lys	7.7	
Ile	8.4	9.4
Leu	19.0	19.2
Tyr	5.7	6.2
Phe	8.4	7.8

[a] The data are expressed as the ratio of residues relative to aspartic acid (set = 22.0).

TABLE III: Sedimentation of a Mixture (1:1 Molar Ratio) of Acetyl-CPA and Succinyl Fraction II.

Sedimentation Velocity: 160 min, 60,000 rpm, 7°, s'_{20} = 2.80 S Sedimentation Equilibrium (low speed)								
Protein Concn (mg/ml)	pH	Buffer (M)	Speed (rpm)	Time (min)	Temp (°C)	M_w	Distribn throughout Cell	M_z
3.37	7.5	KH_2PO_4 (0.038)–KCl (0.1)	7971	1102	6.8	30,850	28,500–34,200	41,884

M KH_2PO_4–0.25 M KCl (pH 9.5). Sufficient acrylonitrile was added to bring the final concentration to 0.4 M, and the solution was incubated at 0–4° for 7 days. After the reaction, excess reagent was removed by dialysis, and the per cent of activity toward Ac-L-TyrOEt determined after activation. The enzyme was found to be 22.7% active based on a rate constant derived from activated PCP (Behnke *et al.*, 1970), a value in agreement with that determined prior to cyanoethylation (*i.e.*, 22.8%).

In order to determine the degree of substitution, the derivative was subjected to acid hydrolysis and amino acid analysis. As calculated by a loss of residues, 7.5 of 11 lysines and 1–2 of 5 histidines had reacted (Table II). Alternatively, according to Riehm and Scheraga (1966) the total lysine content of the protein should be given by the sum of the remaining lysine and the amount of di- and monocarboxyethyllysine generated. This summation yields 11.5 lysine residues/mole of protein, a value in good agreement with the value for the control, 11.3. Since dicarboxyethyllysine is eluted in the same position as *allo*-isoleucine, correction for this latter residue was obtained from a control (24-hr hydrolysis) and found to be 2.67% of the amount of Ile present. The observed value of Ile was 8.37 residues; thus 0.0267 × 8.37 = 0.22 residue, a value which accounts for the above difference and results in an excellent agreement between experimental and theoretical values. There was no indication of a reaction with groups other than lysine or histidine. Cyanoethyl fraction II was fully capable of forming complex as indicated by the *s* rate of the heavy component ($s_{20,w}$ = 3.75 S).

Succinyl fraction II, before or after treatment with hydroxylamine, will not form a complex with CPA nor will it undergo self-association (Behnke *et al.*, 1970). In fact, a control system in which no association can be detected is a mixture of acetyl-CPA and succinyl fraction II. In Table III an *s* rate is tabulated for a 1:1 mixture (molar basis) of acetyl-CPA and succinyl fraction II together with a summary of a low speed sedimentation equilibrium run on the same material. It is evident from the data that this solution behaves as a mixture of nonassociating proteins.

Effect of Modification of CPA on Complex Formation. Effect of Metal. A crystal suspension of apocarboxypeptidase A was mixed with a solution of fraction II (6.6 g/l.) both in the presence and absence of *o*-phenanthroline. The sedimentation velocity patterns in the schlieren optical system appeared typical of complex formation, the *s* rate of the heavy component being 4.17 S in the presence of *o*-phenanthroline and 3.98 S in its absence. Equivalent boundary calculations on an equimolar mixture of fraction II and the CPA derivative (1.27×10^{-4} M) yielded in the presence and absence of *o*-phenanthroline values of 3.39 S. Both sets of data confirm that complex formation had occurred in this system.

The effects of metal replacement in CPA on complex formation were studied by two general methods. Cd-CPA and Hg-CPA crystal suspensions prepared as described under Methods were mixed with fraction II in equimolar ratios or in a 1:1 volume ratio of crystal suspension to fraction II. In each case a solvent system consisting of 0.1 M Tris-HCl (pH 7.0) was used. For the first type of samples mass transport and equivalent boundary sedimentation coefficient values were determined. For the second type of solutions the movement of the maximum ordinate was followed in the ultracentrifuge. The data are presented in Table IV.

From these data it appears that metal replacement does not impair the complex-forming ability of CPA. The second moment and mass transport values are lower than the corresponding schlieren data, again since the former take into account any lighter material present, while the latter tend to weight the heavy component. Rupley and Neurath (1960) reported that the sedimentation properties of apoCPA are identical with that of the native enzyme, and therefore,

TABLE IV: Sedimentation Characteristics of Cadmium and Mercury CPA in the Presence of Fraction II.

Derivative	System	Mass Transport	($s_{20,w}$) Equiv Boundary (S)	Max. Ordinate
Control	Excess crystals of CPA			4.0
CPA	1:1 molar ratio	3.03	3.30	3.94
Cd-CPA + Fraction II ($C = 1.86 \times 10^{-4}$ M)	Excess crystals 1:1 molar ratio	3.31	3.31	4.96
Hg-CPA + fraction II ($C = 2.13 \times 10^{-4}$ M)	Excess crystals 1:1 molar ratio	3.40	3.62	4.36

TABLE V: Amino Acid Composition of Cyanoethyl-CPA.[a]

Amino Acids	24-hr Hydrolysis	CPA (Native)
Lys	5.1	15.0
His	6.0	8.0
Arg	10.6	11.0
Asp	28.7	28.0
Thr	24.0[b]	28.0
Ser	27.6[b]	33.0
Glu	26.0	25.0
Pro	10.9	10.0
Gly	22.2	22.5
Ala	*20.0*	*20.0*
½-Cys	1.9	2.0
Val	15.4[c]	16.0
Met	2.7	3.0
Dicarboxyethyl-Lys	8.6	
Ile	17.8[c]	20.0
Leu	23.4	23.0
Tyr	17.4	19.0
Phe	15.1	16.0
Monocarboxyethyl-Lys	0.6	

[a] The data are corrected to a value of 20.0 alanine residues. [b] Values were not extrapolated to zero time of hydrolysis. [c] Valine and isoleucine were not corrected for the time of hydrolysis.

the heavy component is most probably a complex of the CPA derivative and fraction II rather than an aggregate of the former.

Acetylation of CPA with *N*-acetylimidazole in the presence and absence of β-phenylpropionate was carried out (Simpson *et al.*, 1963) using a 120-fold molar excess of *N*-acetylimidazole and the following buffer system: 0.01 M KH_2PO_4–1 M NaCl (pH 7.5). Modification in the absence of β-phenylpropionate caused a 600% increase in esterase activity compared to the control while peptidase activity fell to 5.6%. β-Phenylpropionate at concentrations between 5×10^{-2} and 0.5 M completely protected the enzyme against these changes. Only partial protection was afforded by β-phenylpropionate at 10^{-3} M.

After acetylation, the solutions were dialyzed at 0–4° for 48 hr against 0.038 M KH_2PO_4–0.1 M KCl (pH 7.5) and tested for their ability to form a complex with fraction II. All the solutions were found to be capable of forming complex (s_{20} = 3.52–3.60 S for the heavy component). Therefore, the active site tyrosyl residues as well as a number of "surface" tyrosines of CPA can be excluded from participation (at least through the OH group) in complex formation.

Cyanoethylation of CPA with acrylonitrile was carried out under the same conditions specified for modification of fraction II. As calculated by a loss of amino acid residues (Table V) 9.9 of 15 lysines and 3 of 8 histidines were substituted. Alternatively, the sum of the remaining lysine plus the sum of the number of dicarboxyethyl- and monocarboxyethyllysines generated should yield the total number of lysines present in the native enzyme. This sum minus a correction for *allo*-isoleucine yielded 13.8, a value approaching the theoretical number of lysines in the protein (15.0). There were no indications of a reaction with groups other than lysine and histidine. The esterase activity of cyanoethyl-CPA rose to a value of 201%, as assayed with 0.01 M HPLA, using rate constants for the native enzyme (Cox *et al.*, 1964). As determined by sedimentation velocity in the ultracentrifuge, the cyanoethyl derivative of CPA does *not* form a complex with fraction II. $s_{20,w}$ calculated from the maximum ordinate positions was 3.35 S.

Nitrocarboxypeptidase was prepared under conditions published by Riordan *et al.* (1967). CPA (12.8 mg) was dissolved in 1.0 ml of 0.05 M Tris-HCl–1 M NaCl (pH 8.0) and treated with a 4-fold molar excess of TNM. The mixture was incubated for 45 min at 20°. Excess reagent was removed by exhaustive dialysis against water. Esterase and peptidase activities were measured and found to be 181 and 22.1% of the control. Absorbance measurements at 381 nm (an isosbestic point for NO_2-tyrosine absorption) indicated 1.17 NO_2-tyrosine groups/mole of CPA using a molar absorbancy index ε of 2200 (Sokolovsky *et al.*, 1966). The nitrated enzyme after dialysis against 0.038 M KH_2PO_4–0.1 M KCl (pH 7.5) exhibited an $s_{20,w}$ of 7.3 S (1.79 mg/ml) indicative of marked self-polymerization ($s_{20,w}$ for a CPA control = 3.31 S). Complex formation with fraction II, if it occurs, does not appear to compete effectively with this self-association of nitro-CPA.

Discussion

Ultracentrifuge techniques have proved useful in the present investigation to analyze the complex formation of CPA and fraction II, and to determine the effects of various modifications of each component on their association with one another.

Weight-average sedimentation coefficients have been used in the past for calculations of chemical equilibria (Schachman, 1959; Steinberg and Schachman, 1966) but previously their role has been in computations involving small molecule–macromolecule interactions or self-associations (Gilbert and Gilbert, 1962). In this investigation a combination of velocity and sedimentation equilibrium calculations has yielded a simple, rapid, and nearly unequivocal method for characterization of hybridization reactions of macromolecules.

The method of continuous variations applied to the sedimentation velocity experiments described in this study provides strong evidence that the complex has a stoichiometry of F_1P_1. This conclusion is made more certain by the high-speed sedimentation equilibrium experiments, which consistently fit the F_1P_1 model better than other models.

Molecular weights of complex for the most part fit within the "allowed space" of F_1, P_1, and F_1P_1. Hence, it may well be that the complex is very tight, sequestering virtually all molecules of F_1 capable of associating either with themselves or with CPA. The remaining molecules might be incapable of participating in any chemical equilibria of this sort. While it should be possible to detect such a mechanism experimentally, no investigation of this type was performed. Because of this possibility we regard the association constant of 2.9×10^4 M^{-1} as an indication of the order of magnitude of the macroscopic association process rather than a true

equilibrium constant. The situation is further complicated by the presence of small amounts of light material. Simulation calculations on self-associating systems (Teller *et al.*, 1969; T. A. Horbett and D. C. Teller, unpublished data) reveal that as little as 5% contamination of a dimerizing system by small molecular weight components can change observed equilibrium constants by as much as a factor or two. Since CPA used in this study was slightly inhomogeneous in exactly this way, it is almost certain that the true equilibrium constant for complex formation is larger than that used in the calculation of the Job plot.

In a paper by Kegeles *et al.* (1967) on the sedimentation behavior of chemically reacting systems, it was stated that in high-speed sedimentation velocity experiments high pressures of the order of 100–500 atm may be generated at the cell base. It has been shown that the gradient of the logarithm of the equilibrium constant follows the molar volume of reaction, which leads to large pressure effects for reacting macromolecules at high speeds. The sedimentation velocity experiments reported here are representative of a number of runs performed at various speeds and concentrations. In no case was there evidence of convection or other indications of boundary instability or anomalies. Ionic bond formation involves the largest volume change among noncovalent interactions between molecules (Linderstrøm-Lang and Jacobsen, 1941). In the case of noncovalent interactions without structural changes, pressure favors the dissociation of macromolecular aggregates. In the experiments reported here, the equilibrium constant derived at low pressure (less than 30 atm) can be applied to the Job plot which was derived from experiments at very high pressures. Thus, within the limits of the errors of the parameters involved, pressure effects were negligible in these experiments.

Table VI summarizes the sedimentation velocity experiments which were used as the principal assay system for the determination of complex formation. Since this assay is rather insensitive to minor differences in association constants for complex formation, the entries in this table should be regarded only as a first approximation to the behavior of these solutions.

Substrates and competitive inhibitors of fraction II are without effect upon formation of a complex. Treatment of fraction II with DFP does not modify the sedimentation velocity patterns, but only 14% of fraction II molecules are capable of reacting with this inhibitor. The sedimentation velocity technique is probably not sufficiently sensitive to determine if this proportion of molecules is incapable of forming a complex. From Table VI it may be seen that activation of fraction II also has no effect upon complex formation. However, this, too, does not exclude overlapping sites for activity and binding to CPA since the proportion of molecules releasing peptides, if any, upon treatment with a trypsin is unknown. At this point it is not possible to make a categorical statement concerning the potential overlap of the active site and the CPA binding site of fraction II.

Consideration of the role of the active site of CPA relative to its binding for fraction II yields the conclusion that these are *not* overlapping areas of the molecular surface. β-Phenylpropionate does not affect complex formation. Complex formation is also independent of the activity in that the presence or absence of a metal ion does not affect the physical system. Replacement of zinc by cadmium or mercury does not eliminate the association; however, its details might be changed (Table VI). Acetylation of 6–7 tyrosyl residues, while modifying the activity of the enzyme, also has no effect on complex formation. Thus, it may be concluded that the binding site of CPA for fraction II is separate from the residues composing the active site.

TABLE VI: Summary of Treatments and Their Effects on Complex Formation.

Treatment	Effect on Complex Formation[a]
Temperature variation	No effect
pH (6.5–8.5)	No effect
Salt concentration increase (1 M)	Decrease complex
Salt concentration decrease (0.05 M)	Decrease complex
Proflavin	No effect
β-Phenylpropionate	No effect
Ac-L-TyrOEt	No effect
DIP fraction II	No effect
Activation of fraction II	No effect
Cyanoethyl fraction II	No effect
Succinyl fraction II	No complex formed
ApoCPA	No effect
Acetyl-CPA	No effect
Cyanoethyl-CPA	No complex formed
Nitro-CPA	Self-associates, complex does not compete effectively

[a] Note that "no effect" is interpreted to be within the sensitivity of the sedimentation velocity assay system for complex formation.

It may be seen from Table VI that succinylation of fraction II precludes formation of complex as does cyanoethylation of CPA. Conversion of the positively charged lysine residues of fraction II to neutral residues has no effect, but conversion of the positively charged lysines to negatively charged succinyllysyl residues has a large effect. It is not known whether the same residues are involved in the two modifications. In CPA cyanoethylation of 10 lysyl and 2 histidyl residues also results in a loss of complex-forming ability. These two modifications of charged residues, the decrease of complex formation in high salt, and the lack of a strong temperature dependence may all be taken as an indication that one of the major driving forces of complex formation is electrostatic interactions between the two proteins.

In a companion paper of this series (Behnke *et al.*, 1970) evidence is presented that fractions II and III derived from the disaggregation of PCP A-S6 are structurally similar, implying that in the trimeric zymogen fractions II and III may be identical subunits. If this is true, then it might be expected that the combination of CPA and fraction III would yield a trimer analogous to PCP A-S6 instead of a dimeric complex. Yet CPA is not equivalent to subunit I but actually is generated from subunit I by the release of

60 amino acid residues (Freisheim *et al.*, 1967). It is possible, therefore, that CPA possesses only one subunit binding site and that the activation peptide of subunit I constitutes or confers a second binding site. It has been suggested (Brown *et al.*, 1963) that this binding site accounts for the slow activation of PCP A-S6. The present results are compatible with such a hypothesis.

Appendix

Job's Method of Continuous Variations with Self-Association of One Component. In the usual method of continuous variations (Woldbye, 1955) there is only a single reaction—that of complex formation. In biochemical equilibrium systems, however, there may be several competing reactions or lack of reactions (incompetent monomers) which interfere with the chemical equilibria.

In the case of fraction II the molecular weight distributions can be adequately described by an indefinite association with identical equilibrium constants. This scheme for association of fraction II (denoted by F) is

$$\begin{aligned} 2F_1 &\rightleftharpoons F_2 & k_1 &= [F_2]/[F_1]^2 \\ F_2 + F &\rightleftharpoons F_3 & k_2 &= [F_3]/[F_2][F_1] \\ &\cdots & &\cdots\cdots \\ F_j + F &\rightleftharpoons F_{j+1} & k_j &= [F_j{}^{+1}]/[F_j][F_1] \end{aligned}$$

and that $k = k_1 = k_2 = \ldots = k_j$. Mixing various volumes, x, of equimolar stock solutions of F and CPA (denoted by P) will then be described by the expressions

$$K[F]^m[P]^n = [F_mP_n] \quad (1)$$

$$C_0x = [P] + n[F_mP_n] \quad (2)$$

$$C_0(1 - x) = m[F_mP_n] + [F]\{1 + 2k[F] + 3(k[F])^2 + \ldots\}$$

or, by condensing the infinite series in [F]

$$C_0(1 - x) = m[F_mP_n] + \frac{[F]}{(1 - k[F])^2} \quad (3)$$

Differentiation of eq 1–3 with respect to x followed by setting $d[F_mP_n]/dx = 0$ to find the position of the maximum ordinate yields

$$m[P]\frac{d[F]}{dx} + n[F]\frac{d[P]}{dx} = 0 \quad (4)$$

$$\frac{d[P]}{dx} = C_0 \quad (5)$$

$$\frac{d[F]}{dx} = -C_0\frac{(1 - k[F])^3}{1 + k[F]} \quad (6)$$

Substitution of eq 5 and 6 into 4 provides an expression for [P] as a function of [F],

$$[P] = \frac{n}{m}[F]\frac{1 + k[F]}{(1 - k[F])^3} \quad (7)$$

This relation may be placed into eq 2 and the simultaneous pair of eq 2 and 3 can be used to find the position of maximum ordinate

$$x = \frac{n}{n + m} + \frac{nk[F]}{n + m}\left\{\frac{n - m}{n}x + 1 - \frac{2m[F_mP_n]}{C_0}\right\} \quad (8)$$

The first term in this equation is the usual expression for the position of the maximum ordinate, while the second term describes the perturbation due to the competing equilibria. Under the conditions such that $n = m$ and $k[F]$ is small then $x \approx 1/2$ and the stoichiometry can be determined. The causes for failure of the experiment would be $n \neq m$, large $k[F]$, or large $m[F_mP_n]/C_0$.

Sedimentation Equilibrium of a System with Complex Formation. In sedimentation equilibrium of a single material which self-associates, the concentration distribution is given by Teller *et al.* (1969)

$$C = C_{p1}\Gamma + C_{p2}\Gamma^2 + C_{p3}\Gamma^3 + \ldots \quad (9)$$

where the C_{pi} are concentrations of the individual species at an arbitrary position, r_p, in the cell, $\Gamma = \exp[\hat{A}M_i(r^2 - r_p{}^2)]$, $\hat{A} = (1 - \bar{v}\rho)\omega^2/2RT$, where $\bar{v}$ is the partial specific volume, ρ is the solution density, ω the angular velocity, R the gas constant, and T the absolute temperature.

In order to study the formation of a complex between two unlike species we need only extend the analysis of the concentration data. The reaction schemes which potentially are possible for CPA fraction systems are

$$6F \rightleftharpoons 3F_2 \rightleftharpoons 2F_3$$

for fraction II and assuming formation of higher polymers would be within experimental error of curve fitting

$$6P_1 \rightleftharpoons 3P_2 \rightleftharpoons 2P_3$$

for CPA.

The formation of complexes would appear to favor the following three possibilities

$$P_1 + F_1 \rightleftharpoons P_1F_1$$

$$2P_1 + F_1 \rightleftharpoons P_2F_1$$

$$P_1 + 2F_1 \rightleftharpoons P_1F_2$$

in the ultracentrifuge

$$C_F = \sum_{k=1}^{3} C_{p,F,k}\Gamma_F{}^k$$

$$C_P = \sum_{j=1}^{3} C_{p,F,j}\Gamma_P{}^j$$

and the total concentration distribution which we consider is

$$C = \sum_{k=1}^{3} C_{p,F,k}\Gamma_P{}^k + \sum_{j=1}^{3} C_{p,P,j}\Gamma_P{}^j + C_{p,F_1P_1}\Gamma_F\Gamma_P + C_{p,F_1P_2}\Gamma_F\Gamma_P{}^2 + C_{p,F_2P_1}\Gamma_F{}^2\Gamma_P \quad (10)$$

TABLE IA: Illustrative Calculations on Model Data.[a]

Composition: Set	A(1)B(0)	A(0)B(1)	A(1)B(1)	A(2)B(0)	A(0)B(2)	A(2)B(1)	A(1)B(2)	RMS Fit		
								M_n	M_w	C
1	+	−	−	+	+	−	+	146,223	97,938	142.639
2	+	+	+	−	−	+	0	9,337	156,622	4.637
3	+	+	+	−	−	0	+	3,641	4,282	5.128
4	+	+	+	+	+	0	0	143	136	0.105
5	+	+	+	−	0	−	+	1,000	982	0.701
6	+	+	+	+	0	+	0	122	107	0.082
7	+	+	+	−	0	0	0	3	3	0.004
8	+	+	−	0	+	−	+	7,313	10,627	6.481
9	+	+	+	0	−	0	+	11	22	0.005
10	+	+	+	0	+	0	0	2	2	0.003
*11	+	+	+	0	0	0	0	2	2	0.000
12	−	+	0	0	0	0	+	95,076	502,352	0.097
13	−	+	0	0	0	+	0	19,014	10,492	0.071
14	+	+	0	0	0	+	−	2,028	1,895	0.014

[a] M_w (A) = 27,000, M_w (B) = 40,000. − = negative coefficients for C_p. + = positive coefficients for C_p. 0 = assumed absent in composition. The asterisk indicates the correct solution.

This expression is linear in the C_p parameters so that it is readily amenable to least-squares curve-fitting procedures. After calculation of the C_p values the equilibrium constants can be obtained from appropriate expressions, for example, for F_1P_1 we have

$$k_{FP} = \left(\frac{M_F M_P}{M_F + M_P}\right) 4.0\left(\frac{C_{p,F_1P_1}}{C_{c,F},\ C_{p,P}}\right)$$

where the units of C_p are fringe values and the factor 4.0 arises from the assumed value of 4.0 fringe l. g^{-1}.

Since so many possibilities exist for combinations of species present, fourteen different solution compositions were tested in two separate computer programs. The first set of possible species included F_1, P_1, F_1P_1, F_2, P_2, F_2P_1, and F_1P_2. The second program replaced P_2 by F_3. Table IA illustrates the calculations for perfect data in a simulated system using the first program. The physical constraints which are applied to this system are: (1) all calculated C_p values must be positive, (2) the back-calculated concentration values of the components must be consistent with the proposed model, and (3) the back-calculated weight- and number-average molecular weights must be consistent with the observed data.

In Table IA for the model data the only possible real solutions are sets 4, 6, 10, and 11. While set 11 is the correct answer and gave correct values of the constants, it is almost indistinguishable from set 10 which included a small amount of F_2 as well as the correct complex. It should be noted that these computations are based on perfect data and any real data would be expected to show more ambiguity.

Simulation of a Rayleigh Interferogram. In order to simulate the sedimentation equilibrium pattern of a mixture of self-associating fraction II and CPA monomer in which complex formation was assumed absent, the following theory was employed.

The concentration of a homogeneous, ideal component at sedimentation equilibrium in a high-speed sedimentation equilibrium experiment will be given by the relation (Teller *et al.*, 1969)

$$C_i = C_{0,i}H_i e^{(\psi+1)H_i}/\sinh H_i \simeq 2C_{0,i}H_i e^{\psi H_i} \qquad (11)$$

where i refers to the ith component, $C_{0,i}$ is the mass-average concentration

$$\int_{r_m}^{r_b} C\mathrm{d}(r^2) \Big/ \int_{r_m}^{r_b} \mathrm{d}(r^2)$$

$$H_i = \frac{(1 - v\rho)\omega^2}{4RT} M_i(r_b^2 - r_m^2)$$

$$\psi = 2(r^2 - r_b^2)/(r_b^2 - r_m^2)$$

In eq 10, the first equality is exact (van Holde and Baldwin, 1958) while the approximation on the right follows by assuming $H_i > 2$ so that $\sinh H_i \simeq e^{H_i}/2$. Physically this means that the meniscus concentration is negligible. A sectorial cell is assumed for the derivation of eq 11.

The quantities $2C_{0,i}H_i$ are identical with the concentrations at the cell base, $C_{b,i}$. The values of the $C_{0,i}$ represent the initial compositions of a hypothetical solution, not in chemical equilibrium, which would have been observed if a non-equilibrium mixture of proteins had been combined and centrifuged at the same speed.

For an indefinite self-association the concentrations of species other than monomer are given by

$$C_i = iK^{(i-1)}C_1^{\,i} \qquad (12)$$

where $K = k/M_1$ and has units of liters per gram: the concentration units are thus g/l. The relation between $C_{0,i}$ values follows from eq 11 and 12

$$C_{0,i} = (2KC_{0,i}H_1)^{i-1}C_{0,i}\ i = 2, 3, \ldots . \quad (13)$$

Since C_0, which is the total mass-average concentration, is the sum of the $C_{0,i}$, it follows that $C_0 = C_{0,i}/(1 - 2KC_{0,i}H_1)$ or, solving for $C_{0,1}$ we obtain

$$C_{0,1} = C_0/(1 + 2KC_0H_1) \quad (14)$$

Equation 14 gives the relation between the total initial concentration of the self-associating material and the mass-average concentration of monomer, while eq 13 provides the mass-average concentrations of the remaining species participating in the indefinite association.

It must be emphasized that these concentrations never actually exist. They are defined by the total mass of monomers, dimers, etc., at sedimentation equilibrium. As stated above the solution is hypothetical prior to distribution; nevertheless, it will give the correct distribution for a chemically reacting system at sedimentation equilibrium.

For the actual simulation of the sedimentation equilibrium diagram of a mixture of CPA and self-associating fraction II, C_0 values for CPA and fraction II (all species) were assumed. From eq 12 and 13 the amounts of fraction II nonamer, dimer, etc., were calculated using $M_1 = 2.287 \times 10^4$ g/mole and $k = 8.6 \times 10^3$ l./mole (Teller, 1970). Beyond monomer the concentrations of remaining species were negligible (weight fraction less than 10^{-5}). The exact equality in eq 10 was then used to compute the total concentration at 50 equally spaced points of ψ. Positions of integral fringe numbers were determined by quadratic interpolation using a slight modification of the computer program described by Teller (1965). Number-, weight-, and Z-average molecular weights at each concentration were calculated by the usual relations (Schachman, 1959). These predicted molecular weight moments were plotted as shown in the text (Figure 2) to prove that hybrid species are present in mixtures of CPA and fraction II.

References

Adams, E. T., Jr. (1964), *Proc. Nat. Acad. Sci. U. S. 51*, 509.

Behnke, W. D., Wade, R. D., and Neurath, H. (1970), *Biochemistry 9*, 4179.

Brown, J. R., Greenshield, R. N., Yamasaki, M., and Neurath, H. (1963), *Biochemistry 2*, 867.

Coleman, J. E., and Vallee, B. L. (1960), *J. Biol. Chem. 235*, 390.

Cox, D. J., Bovard, F. C., Bargetzi, J.-P., Walsh, K. A., and Neurath, H. (1964), *Biochemistry 3*, 44.

Dixon, M., and Webb, E. C. (1964), Enzymes, New York, N. Y., Academic, p 326.

Doty, P., and Edsall, J. T. (1951), *Advan. Protein Chem. 6*, 35.

Freisheim, J. H., Walsh, K. A., and Neurath, H. (1967), *Biochemistry 6*, 3020.

Gilbert, L. M., and Gilbert, G. A. (1962), *Nature 194*, 1173.

Glazer, A. N. (1965), *Proc. Nat. Acad. Sci. U. S. 54*, 171.

Kegeles, G., Rhodes, L., and Bethune, J. L. (1967), *Proc. Nat. Acad. Sci. U. S. 58*, 45.

Lansing, W. D., and Kraemer, E. O. (1935), *J. Amer. Chem. Soc. 57*, 1369.

Linderstrøm-Lang, K., and Jacobsen, C. F. (1941), *C. R. Trav. Lab. Carlsberg 24*, 1.

Massie, B. B., Titchener, E. B., and Hanlon, S. (1968), *Arch. Biochem. Biophys. 128*, 753.

McClure, W. O. (1964), Ph.D. Dissertation, University of Washington.

Pétra, P. H., and Neurath, H. (1970), *Biochemistry* (in press).

Richards, E. G., and Schachman, H. K. (1959), *J. Phys. Chem. 63*, 1578.

Riehm, J. P., and Scheraga, H. A. (1966), *Biochemistry 5*, 93.

Riordan, J. F., Sokolovsky, M., and Vallee, B. L. (1967), *Biochemistry 6*, 358.

Rubin, M. M. (1966), Dissertation, University of California, Berkeley.

Rupley, J. A., and Neurath, H. (1960), *J. Biol. Chem. 235*, 609.

Schachman, H. K. (1957), *Methods Enzymol. 4*, 32.

Schachman, H. K.(1959), Ultracentrifugation in Biochemistry, New York, N. Y., Academic.

Simpson, R. T., Riordan, J. F., and Vallee, B. L. (1963), *Biochemistry 2*, 616.

Sokolovsky, M., Riordan, J. F., and Vallee, B. L. (1966), *Biochemistry 5*, 3582.

Steinberg, I. Z., and Schachman, H. K. (1966), *Biochemistry 5*, 3728.

Svennson, H. (1954), *Opt. Acta 1*, 25.

Svennson, H. (1956), *Opt. Acta 3*, 164.

Teller, D. C. (1965), Ph.D. Dissertation, University of California, Berkeley.

Teller, D. C. (1970), *Biochemistry 9*, 4201.

Teller, D. C., Horbett, T. A., Richards, E. G., and Schachman, H. K. (1969), *Ann. N. Y. Acad. Sci. 164*, 66.

van Holde, K. E., and Baldwin, R. L. (1958), *J. Phys. Chem. 62*, 734.

Woldbye, F. (1955), *Acta Chem. Scand. 9*, 299.

Yamasaki, M., Brown, J. R., Cox, D. J., Greenshields, R. N., Wade, R. D., and Neurath, H. (1963), *Biochemistry 2*, 859.

Yphantis, D. A. (1964), *Biochemistry 3*, 297.

Yphantis, D. A., and Roark, D. E. (1969), *Ann. N. Y. Acad. Sci. 164*, 245.